# Reporter–nanobody fusions (RANbodies) as versatile, small, sensitive immunohistochemical reagents

Masahito Yamagata[a,b] and Joshua R. Sanes[a,b,1]

[a]Center for Brain Science, Harvard University, Cambridge MA, 02138; and [b]Department of Molecular and Cellular Biology, Harvard University, Cambridge MA, 02138

Contributed by Joshua R. Sanes, January 11, 2018 (sent for review December 27, 2017; reviewed by Harvey J. Karten and Rachel O. L. Wong)

**Sensitive and specific antibodies are essential for detecting molecules in cells and tissues. However, currently used polyclonal and monoclonal antibodies are often less specific than desired, difficult to produce, and available in limited quantities. A promising recent approach to circumvent these limitations is to employ chemically defined antigen-combining domains called "nanobodies," derived from single-chain camelid antibodies. Here, we used nanobodies to prepare sensitive unimolecular detection reagents by genetically fusing cDNAs encoding nanobodies to enzymatic or antigenic reporters. We call these fusions between a reporter and a nanobody "RANbodies." They can be used to localize epitopes and to amplify signals from fluorescent proteins. They can be generated and purified simply and in unlimited amounts and can be preserved safely and inexpensively in the form of DNA or digital sequence.**

camelid antibody | horseradish peroxidase | GFP | nanobody | retina

Sensitive, specific, and reproducible localization of molecules in cells and tissues is indispensable in many areas of biological inquiry. The most commonly used methods are immunohistochemical. The introduction of the immunofluorescent technique, in which antibodies are conjugated to a fluorophore (1), had a profound influence but suffered from limited sensitivity and specificity, the need to laboriously generate conjugates of each antibody preparation, and the potential loss of activity upon conjugation. These limitations were addressed by refinements of the technology, including affinity purification of monospecific antibodies from sera to improve specificity, the use of enzymatic labels such as horseradish peroxidase to improve sensitivity, and the use of second antibodies (indirect immunofluorescence) to avoid the need for chemical modification of the primary antibody (2, 3).

Nonetheless, difficulties remained. Polyclonal antibodies from immunized animals are often poorly defined, available in limited amounts, and variable from bleed to bleed (4, 5). Some but not all of these problems were addressed by the introduction of monoclonal antibodies generated from hybridomas (6): They are monospecific, molecularly defined, and can be produced in unlimited amounts. However, they are laborious to generate. Moreover, storage of hybridomas is costly and, even at low temperatures, impermanent.

A subsequent step toward routine production of specific and sensitive immunoreagents was the development of methods for selection and generation of recombinant antigen-binding antibody fragments. The first of these were variable regions from conventional antibodies, cloned by PCR and then evolved, and selected by methods such as phage display (7, 8). More recently, single-chain antibodies from camelids (9) or selachians (10) have been used for research, diagnostic, and therapeutic purposes (11). Importantly, the high affinity of the antigen-recognition site in these single-chain molecules is retained in fragments called "nanobodies" that comprise only the ∼130-aa variable domain (12, 13). Nanobodies are thus easy to clone and derivatize by coupling to reporters or dyes (14–17). Moreover, they can be stored with high stability and low cost as cDNAs or regenerated at relatively low cost from a digitally stored sequence.

Here, we report an immunohistochemical platform based on nanobodies. We fuse the nanobody to a reporter and append an epitope tag that enables detection of the protein independent of its bioactivity as well as one-step affinity purification from culture medium. Nanobody sequences can be synthesized and cloned into a destination vector containing all other elements. We call these reagents "RANbodies" for "fusions between a **r**eporter **a**nd a **n**anobody." We describe methods for generating RANbodies using each of four reporters: a variant of horseradish peroxidase, two highly antigenic proteins ("spaghetti monsters") (18), and the Fc fragment of an avian antibody. We document the versatility of these reagents for the detection of antigens in cultured cells and tissues, with an emphasis on amplifying weak signals from multiple fluorescent proteins (XFPs). We believe that the simplicity of the method and specificity of the reagents will make them widely useful.

## Results

**RANbody Platform.** RANbody probes contain the following six elements: (*i*) an N-terminal mammalian signal peptide from the human Ig kappa chain to enable secretion of the protein from cultured cells; (*ii*) a HA epitope tag to enable immunochemical detection of the protein independent of its binding and enzymatic activities; (*iii*) a camelid nanobody; (*iv*) a short linker; (*v*) a reporter; and (*vi*) a His epitope tag to enable one-step affinity purification of the protein from culture medium (Fig. 1 *A* and *B*).

For facile construction of RANbodies, we used the Gibson Assembly method (19) in which multiple overlapping DNA molecules can be assembled in a single step. The nanobody fragments, which are ∼400 bp long, were synthesized commercially, and other components were generated by PCR from readily available plasmids. The resulting vectors were transfected into the mammalian cell

## Significance

**Conventional antibodies are often poorly defined, limited in amount, and difficult to store permanently. Nanobodies, recombinant antigen-binding proteins derived from single-chain camelid antibodies, circumvent many of these limitations. To maximize the potential of nanobodies, we fused them to highly sensitive reporters and appended sequences to enable ready production and purification. These RANbodies (reporter and nanobody fusions) can be readily produced in cultured cells, purified in a single step, used to label cells or tissue, and stored indefinitely in the form of DNA or DNA sequences. Given the rapidly increasing rate of nanobody generation, the RANbody platform provides a versatile and scalable platform for immunohistochemical and biochemical analyses.**

Author contributions: M.Y. and J.R.S. designed research; M.Y. performed research; M.Y. and J.R.S. analyzed data; and M.Y. and J.R.S. wrote the paper.

Reviewers: H.J.K., University of California, San Diego; and R.O.L.W., University of Washington.

The authors declare no conflict of interest.



[1]To whom correspondence should be addressed. Email: sanesj@mcb.harvard.edu.

This article contains supporting information online at www.pnas.org/lookup/suppl/doi:10.1073/pnas.1722491115/-/DCSupplemental.

Published online February 13, 2018.

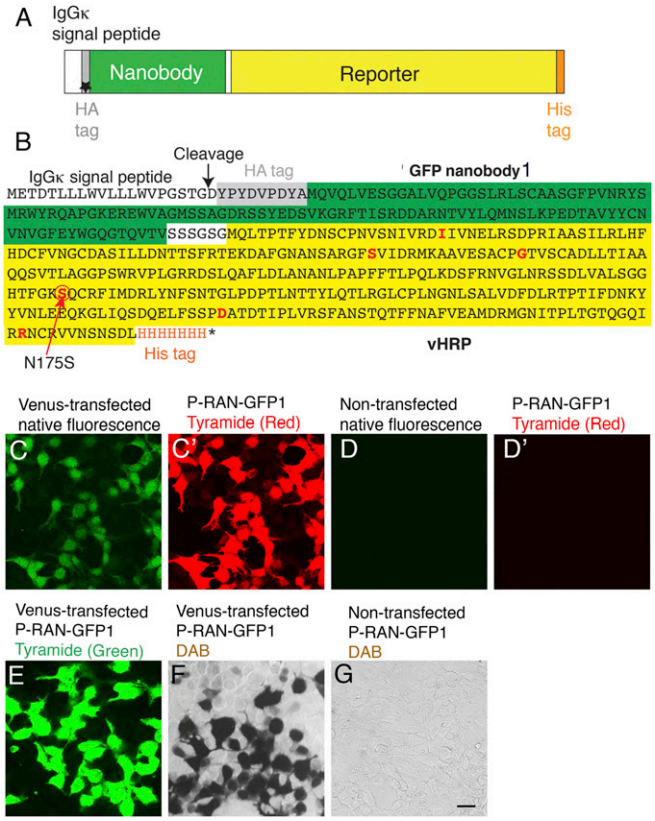


**Fig. 1.** Structure and use of RANbodies. (*A*) RANbody structure. Elements, in order, are (*i*) a mammalian signal sequence, (*ii*) HA epitope tag, (*iii*) nanobody, (*iv*) spacer, (*v*) reporter, (*vi*) stretch of small amino acids, and (*vii*) polyhistidine (His) epitope tag. (*B*) Sequence of P-RAN-GFP1 The reporter is an enhanced variant of HRP (vHRP). Amino acids in red show mutations that enhance activity compared with native HRP; of these N175S has the greatest effect. (*C* and *C′*) RANbody staining. 293T cells transfected with a YFP variant (Venus) were incubated with P-RAN-GFP1 and stained with Cy3-tyramide) (*C*, native fluorescence; *C′*, Cy3 fluorescence). (*D* and *D′*) Untransfected cells stained as in *C*. (*E*) Transfected cells stained as in *C* but with FITC- tyramide. (*F*) Transfected cells stained as in *C* but with a chromogenic substrate, DAB. (*G*) Untransfected cells stained as in *F*. (Scale bar, 10 μm.)

line 293T, and RANbodies were collected from the medium. Diluted culture medium was adequate for staining in most cases. However, by using the His tag at the C terminus, we were able to concentrate the activity by more than two orders of magnitude in a single step on a commercially available affinity resin, as judged by peroxidase activity. The purified recombinant proteins (~450 amino acids) migrated as a single ~60- to 65-kDa band on SDS-polyacrylamide gels (Fig. S1). The larger-than-expected size and diffuse nature of the band likely reflect heterogeneous glycosylation.

**Nomenclature.** We use a simple nomenclature for RANbodies, in which the term "RAN" is preceded by a one-letter abbreviation denoting the reporter and is followed by the antigen to which the nanobody is directed. Reporters described here are HRP (P), HA-tagged spaghetti monster (H), Myc-tagged spaghetti monster (M), and the chicken IgY-Fc region (Y). Thus, a RANbody incorporating a nanobody directed at GFP and horseradish peroxidase is denoted P-RAN-GFP. If there are multiple RANbodies with this design, they can be distinguished by number, for example P-RAN-GFP1, P-RAN-GFP2, and so forth.

**Optimization of HRP as Reporter.** Plant-derived HRP is a highly sensitive and commonly used reporter (20). We therefore initially used HRP as a reporter. To this end, we compared three HRP variants: The first, erHRP, was a "humanized" version of the horseradish protein, with no changes to the amino sequence but with its nucleotide sequence optimized to improve translation efficiency in mammalian cells. An endoplasmic reticulum retention signal was appended to the C terminus to allow folding and glycosylation of the protein, which does not occur in the cytoplasm (21). The second variant, sHRP, bore a single mutation, N175S, which enhances enzyme activity and protein stability (22, 23). The third variant, vHRP, bears five additional point mutations, which were selected to improve the stability of a reconstituted "split HRP" (24) but had not been studied as a single enzyme. All three versions were fused to an HA tag so that protein concentration could be compared. Of the three, vHRP was most active, whether measured histochemically (Fig. S2*A*) or by enzyme assay in solution (Fig. S2 *B* and *C*). This version was therefore used to generate RANbodies of the P series (Fig. 1 *A* and *B* and Table S1).

**P-RANbody: Detection of GFP with HRP-Containing RANbody.** We first generated and purified a RANbody bearing a GFP nanobody described by Kubala et al. (25). Using the nomenclature described above, we refer to this reagent as "P-RAN-GFP1." We used P-RAN-GFP1 to stain 293T cells transfected with Venus, an enhanced YFP (eYFP) modified from *Aequorea victoria* GFP (26). Cells were fixed, permeabilized, incubated with RANbody, and then rinsed and incubated with an HRP substrate. Venus was readily detected using a fluorogenic tyramide substrate with red (Cy3) or green (FITC) fluorescence (Fig. 1 *C*–*E*) or a chromogenic HRP substrate, 3, 3′-diaminobenzidine (DAB), which generates visible brown precipitates (Fig. 1*F*). Untransfected cells were unstained (Fig. 1*G*).

**Comparison of P-RANbody and Antibody Detection.** We compared the sensitivity of P-RAN-GFP1 to intrinsic GFP (Venus) fluorescence and conventional indirect immunofluorescence in two ways. First, we imaged fields of 293T-transfected cells that had been stained with P-RAN-GFP1 and a red tyramide substrate. Some transfected cells were readily identified with the RANbody even though intrinsic fluorescence was barely detectable (Fig. S3*A*). Second, we stained parallel samples with monoclonal or polyclonal antibodies to GFP, followed by an appropriate second antibody or with P-RAN-GFP1 and then imaged them using confocal optics with equal gain (Fig. S3*B*). At the lowest gain, only RANbody-stained cells were visible. At intermediate gain, both RANbody- and antibody-stained cells were visible. Only with the highest gain, when RANbody-stained samples were highly saturated, was intrinsic fluorescence detectable. Comparison of images acquired at the same gain indicated that RANbody increased signals ≥10-fold over antibody staining and ≥100-fold over intrinsic fluorescence. The amplification provided by the HRP/tyramide system is likely to be the major contributor to the increased signal from P-RANbody staining compared with indirect immunofluorescence, but other factors, such as decreased background and the high penetration of the small protein, may also be involved.

**Detection of Cellular Antigens.** To ask whether RANbodies could also be used to localize endogenous proteins, we generated reagents that recognized the histone H2A/H2B heterodimer and the active-binding protein gelsolin using published nanobody sequences (Table S1) (27, 28). Histones are confined to nuclei, and gelsolin is cytoplasmic. As expected, P-RAN-H2A2B stained nuclei and P-RAN-gelsolin stained the cytoplasm in 293T cells using either fluorescent (Fig. 2 *A*–*C*) or colorimetric (Fig. 2*E*) detection.

A key advantage of indirect immunohistochemistry is the ability to visualize multiple antigens in the same cells using antibodies from different species. Although this is not possible using only P-RANbodies, we were able to stain with two P-RANbodies sequentially without cross-reactivity. For this purpose we applied one RANbody, stained with a FITC fluorophore, stripped off the

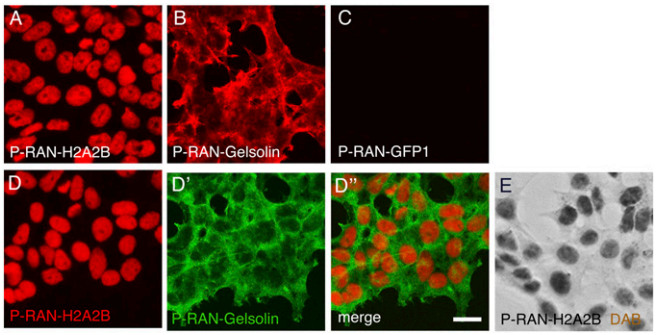


**Fig. 2.** Detection of endogenous proteins with RANbodies. (*A–C*) 293T cells were incubated with P-RAN-H2A2B (*A*), P-RAN-gelsolin (*B*), or P-RAN-GFP1 (*C*) and were stained with Cy3-tyramide for 30 min. Panels were imaged at the same exposure. (*D–D″*) 293T cells were stained with P-RAN-H2A2B/Cy3-tyramide (*D*), stripped with an acidic buffer, and restained with P-RAN-gelsolin/FITC-tyramide (*D′*). Images are merged in *D″*. (*E*) Untransfected cells incubated with P-RAN-H2A2B and stained with DAB. (Scale bar: 10 μm.)

first RANbody with pH 2.0 acidic buffer, and then applied a second RANbody, which we revealed with a Cy3 fluorophore. Fig. 2*D* shows cells doubly stained with P-RAN-H2A2B and P-RAN-gelsolin using this protocol.

**Detection of Multiple XFPs.** We next asked whether RANbodies could be used to amplify signals from XFPs other than GFP and its derivatives (e.g., YFP and Venus). To this end, we generated P-RAN-RFP4, incorporating the nanobody LaM-4 described by Fridy et al. (29). P-RAN-RFP4 stained cells transfected with mCherry (a monomeric RFP modified from *Discosoma* sp. RFP) (30) but did not react with Venus. In contrast, P-RAN-GFP1 stained Venus-transfected but not mCherry-transfected cells (Fig. 3 *A* and *B*).

We also generated two additional RANbodies to RFP, seeking ones that could discriminate among RFPs. All three, P-RAN-RFP2, -RFP4, and -RFP6, derived from LaM-2, -4, and -6, respectively (29), recognized mCherry but differed in their ability to recognize other RFPs: P-RAN-RFP2 was specific for mCherry; P-RAN-RFP4 recognized both mCherry and dsRed2, a variant of *Discosoma* sp. RFP; and P-RAN-RFP6 recognized mCherry, dsRed2, and tdTomato, a tandem dimer of mCherry (Fig. 3 *C–F*).

**RANbody-GFP for GFP Reconstitution Across Synaptic Partners Amplification.** The GFP Reconstitution Across Synaptic Partners (GRASP) method makes use complementation between two fragments of GFP expressed in different cells to label synapses and other sites of intercellular contact (31). Neither of the so-called "split GFP" (sGFP) fragments, sGFP1-10 and sGFP11, is fluorescent on its own, but the reconstituted protein is fluorescent, thus revealing contacts between cells that express different fragments. Because the density of GFP is often low at such sites, the signal is sometimes amplified by use of antibodies that recognize the reconstituted fragment but neither fragment alone (32, 33). However, few such antibodies are available and those that are polyclonal require affinity purification (33). We therefore asked whether RANbodies could serve as reagents to amplify GRASP signals.

P-RAN-GFP1 recognized both sGFP1-10 and GFP. We therefore generated additional RANbodies to GFP based on nanobodies LaG-26 and LaG-41 (Table S1) (29). Both P-RAN-GFP26 and P-RAN-GFP41 stained GFP or Venus approximately as well as P-RAN-GFP1, but neither recognized sGFP1-10–linked neurexin (NRXN) or sGFP11-linked neuroligin-1 (NLGN) (Fig. 4 *A–C*). We cotransfected sGFP1-10 and sGFP11 into 293T cells to enable intracellular complementation (Fig. 4*D*) and used the enzymatic assay described above to compare the specificity of these GFP RANbodies with that of conventional polyclonal and monoclonal antibodies (Fig. 4*E*). The ability of P-RAN-GFP26 and -GFP41 to discriminate reconstituted GFP from its fragments was superior to that of monoclonal and polyclonal antibodies that have previously been used for this purpose (32, 33). Likewise, P-RAN-GFP26 and -GFP41 can recognize reconstituted GFP at cell–cell contacts between sGFP1-10NRXN– and sGFP-11NLGN–transfected cells (Fig. 4 *F* and *G*).

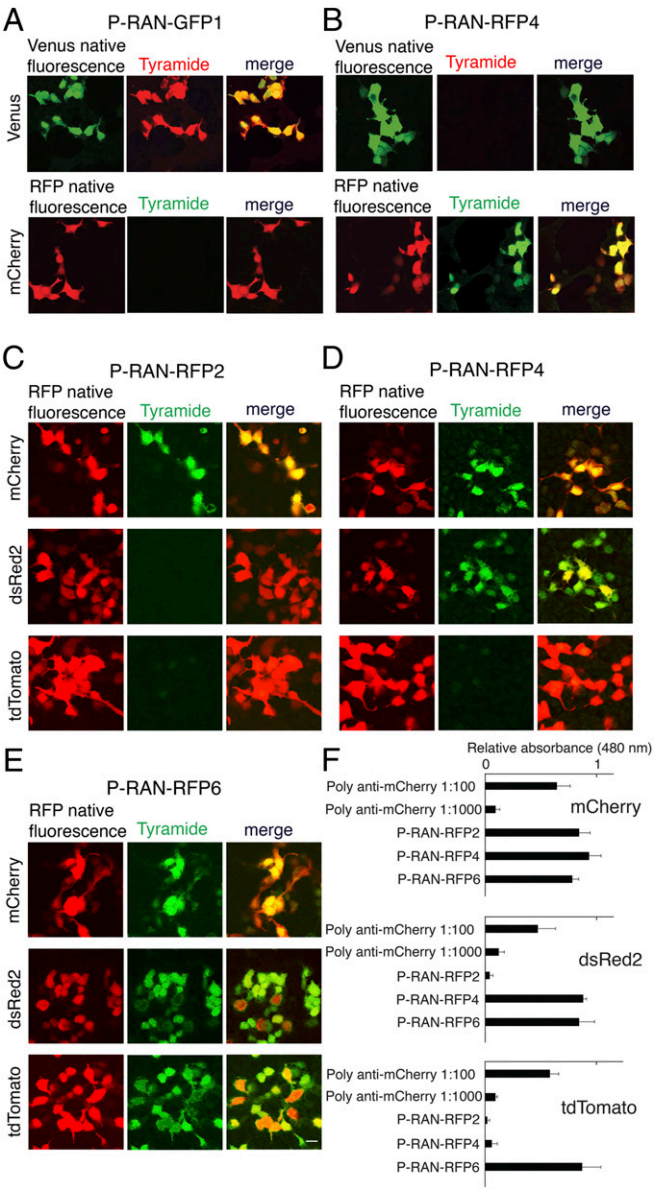


**Fig. 3.** Detection of multiple fluorescent proteins with RANbodies. (*A* and *B*) 293T cells transfected with Venus or mCherry were incubated with P-RAN-GFP1 (*A*) or P-RAN-RFP4 (*B*) and were stained using a Cy3 (red) or FITC (green) tyramide dye. Each RANbody was specific for its cognate antigen. (*C–E*) 293T Cells transfected overexpressing mCherry, dsRed2, or tdTomato (all sea anemone RFP derivatives) were incubated with P-RAN-RFP2 (*C*), P-RAN-RFP4 (*D*), or P-RAN-RFP6 (*E*) and were stained with FITC-tyramide. All P-RAN-RFPs recognize mCherry, but they differ in their ability to detect dsRed2 and tdTomato. (Scale bar, 10 μm.) (*F*) Enzymatic detection of cell-bound RANbodies (as in *C–E*) with a water-soluble substrate provides a second demonstration of the specificity of RFP-RANbodies-P for mCherry, dsRed2, and tdTomato. Rabbit anti-RFP polyclonal antibodies react to all the RFP variants. Data are shown as mean ± SEM, $n = 3$.

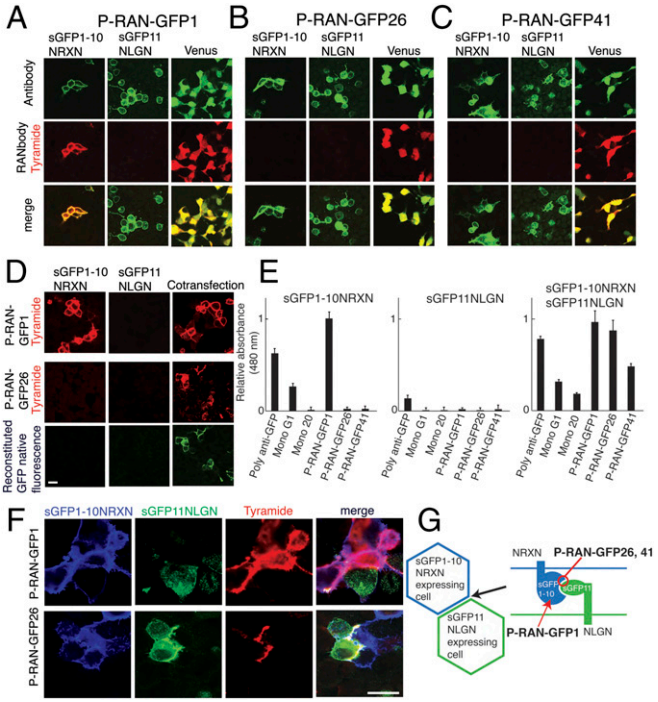


**Fig. 4.** RANbodies-GFP distinguish reconstituted GFP from GFP fragments. (*A–C*) Cells transfected with the 1–10 fragment of GFP fused to neurexin (sGFP1-10NRXN; NRXN), the short fragment of GFP fused to neuroligin (sGFP11NLGN; NLGN), or Venus (holo-YFP; Venus) were incubated with P-RAN-GFP1 (*A*), P-RAN-GFP26 (*B*), or P-RAN-GFP41 (*C*) and were stained with Cy3-tyramide. sGFP1-10NRXN and sGFP11NLGN were detected with anti-NRXN1β and anti-NLGN1, respectively. All three RAN-GFPs recognize Venus. P-RAN-GFP1 (*A*) also recognized sGFP1-10, but not sGFP11. P-RAN-GFP26 (*B*) and -GFP41 (*C*) do not recognize either fragment. (*D*) sGFP1-10NRXN and sGFP11NLGN plasmids were transfected individually or were cotransfected. In the cotransfected cells, reconstituted GFP exhibited green fluorescence and was recognized by P-RAN-GFP26 as well as P-RAN-GFP1 (Cy3-tyramide). (*E*) Enzymatic assay using a water-soluble HRP substrate confirmed differential reactivity of P-GFP-RANs with sGFP1-10NRXN, sGFP11NLGN, and reconstituted (cotransfected) GFP (mean ± SEM, $n = 3$). Mouse monoclonal antibody clone #20 (Mono 20) is selective for reconstituted GFP, whereas the monoclonal antibody GFP-G1 and a rabbit anti-GFP polyclonal antibody also detect sGFP1-10. (*F*) P-RAN-GFP26 was used to detect the reconstituted GFP generated *in trans* at points of contact between cells transfected with sGFP1-10NRXN and sGFP11NLGN and then mixed. P-RAN-GFP1 also stained sGFP1-10NRXN–transfected cells. sGFP1-10NRXN and sGFP11NLGN were detected with chicken anti-GFP (blue) and anti-NLGN1 (green), respectively. (*G*) Schematic of results shown in *F*. (Scale bar in *D*: 10 μm for *A–D*; scale bar in *F*: 10 μm.)

**H- and M-RANbodies: RANbodies Incorporating Highly Antigenic Reporters.** Although P-RANbodies incorporating HRP are useful reagents, there are cases in which enzymatic reactions are inconvenient. In addition, tyramide reagents are costly, and colorimetric reagents are difficult to incorporate into double- or triple-labeling protocols. We therefore asked whether the HA epitope tag contained in the P-RANbodies (Fig. 1*A*) could be used for immunofluorescent detection. We incubated tdTomato-transfected 293T cells with P-RAN-RFP6 and then used a Dylight488-conjugated anti-HA tag antibody to stain the cells. Staining was specific but dim (Fig. 5*B*). We therefore generated a new set of RANbodies that incorporated highly antigenic reporters, spaghetti monsters (18), in place of HRP (Fig. 5*A*). These reporters incorporate 10 HA or MYC epitope tags in a GFP scaffold; we call them "H-RANbodies" and "M-RANbodies," respectively. As shown in Fig. 5 *C*, *D*, *M*, *N*, and *P*, these reporters enabled sensitive detection of RFP and histone (H-RAN-RFP6, H-RAN-H2A2B, and M-RAN-H2A2B) by either direct detection using dye-coupled anti-HA antibody or indirect staining with dye-conjugated secondary antibodies. Of the GFP RANbodies tested, most were ineffective because they recognized epitopes in the scaffold (e.g., Fig. 5*G*). However, H-RAN-GFP1 did not recognize the scaffold and was therefore useful for detecting GFP and its derivatives (e.g., Venus) in tissues (Fig. 5*F*).

**Y-RANbody: RANbodies Incorporating a Chicken Fc Fragment.** In many cases, mouse or rat monoclonal and rabbit polyclonal antibodies are the only available reagents for detecting antigens in tissue. Detection of additional antigens with conventional second antibodies therefore requires the use of antibodies derived from other species. To expand the possibilities for multiple labeling, we used an Fc fragment of chicken IgY as a reporter (Fig. 5*I*). This Fc3-4 fragment contains two Ig domains, which can be detected with readily available fluorophore-coupled secondary antibodies to chicken IgY (Fig. 5 *J*, *K*, *L*, and *Q*). Indeed, RANbodies incorporating this reporter, Y-RAN-RFP6, Y-RAN-GFP1, Y-RAN-GFP26, and Y-RAN-H2A2B, were approximately as sensitive as RANbodies incorporating spaghetti monsters as reporters (Fig. 5). Moreover, unlike spaghetti monster-derived

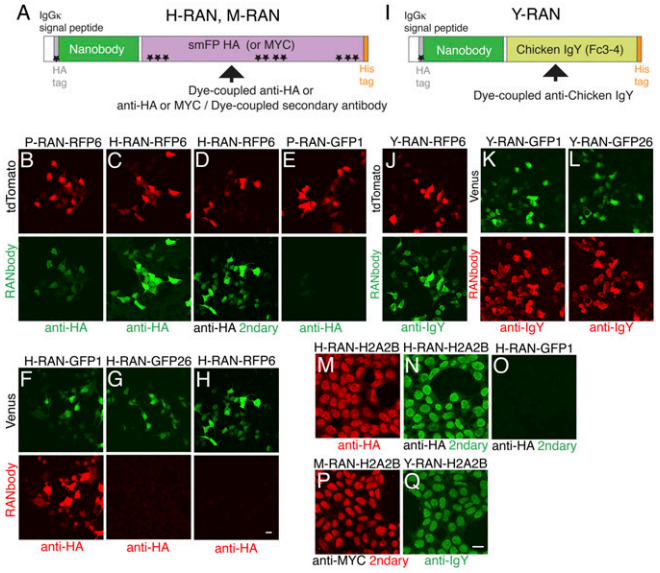


**Fig. 5.** RANbodies incorporating epitope-tagged and antibody-based reporters. (*A*) Structure of H- and M-RANbodies, incorporating 10 HA or MYC epitope tags, respectively, in a GFP scaffold (spaghetti monster) (18). These reporters can be stained with antibodies to the HA and MYC epitopes. Note that P-RANbody incorporates a single HA tag. (*B–E*) Detection of tdTomato in 293T cells with P-RAN-RFP6 (with one HA tag) and Dylight488-coupled anti-HA (*B*), H-RAN-RFP6 (with 11 HA tags) and Dylight488-coupled mouse monoclonal antibody to HA tag (*C*) or H-RAN-RFP6, unconjugated rat monoclonal antibody to HA tag and second antibody (*D*). As a control, tdTomato-transfected cells were incubated with P-RAN-GFP1 and stained with Dylight488-coupled anti-HA (*E*). All the images were obtained with the same gain. (*F–H*) Venus expressing in 293T cells were incubated with H-RAN-GFP1 (*F*), H-RAN-GFP26 (*G*), or H-RAN-RFP6 (*H*) and were stained with Alexa Fluor 555-coupled anti-HA antibody. H-RAN-GFP1 stained Venus, but H-RAN-GFP26 stained poorly because the nanobody recognized the spaghetti monster reporter. (*I*) Structure of Y-RANbodies incorporating the Fc3-4 segment of Chicken IgY as reporter. Fc3-4 can be stained with fluorophore-coupled antibodies to chicken IgY. (*J–L*) Detection of tdTomato and Venus in 293T cells with Y series RANbodies stained with fluorophore-conjugated anti-chicken IgY: Y-RAN-RFP6 (*J*), Y-RAN-GFP1 (*K*), and Y-RAN-GFP26 (*L*). (*M–Q*) Detection of histone in untransfected 293T cells with H-RAN-H2A2B (*M* and *N*), M-RAN-H2A2B (*P*), and Y-RAN-H2A2B (*Q*), stained as in *C–H*. H-RAN-GFP1 (*O*) serves as a negative control. (Scale bar in *H*: 10 μm for *B–H*; scale bar in *Q*: 10 μm for *M–Q*.)

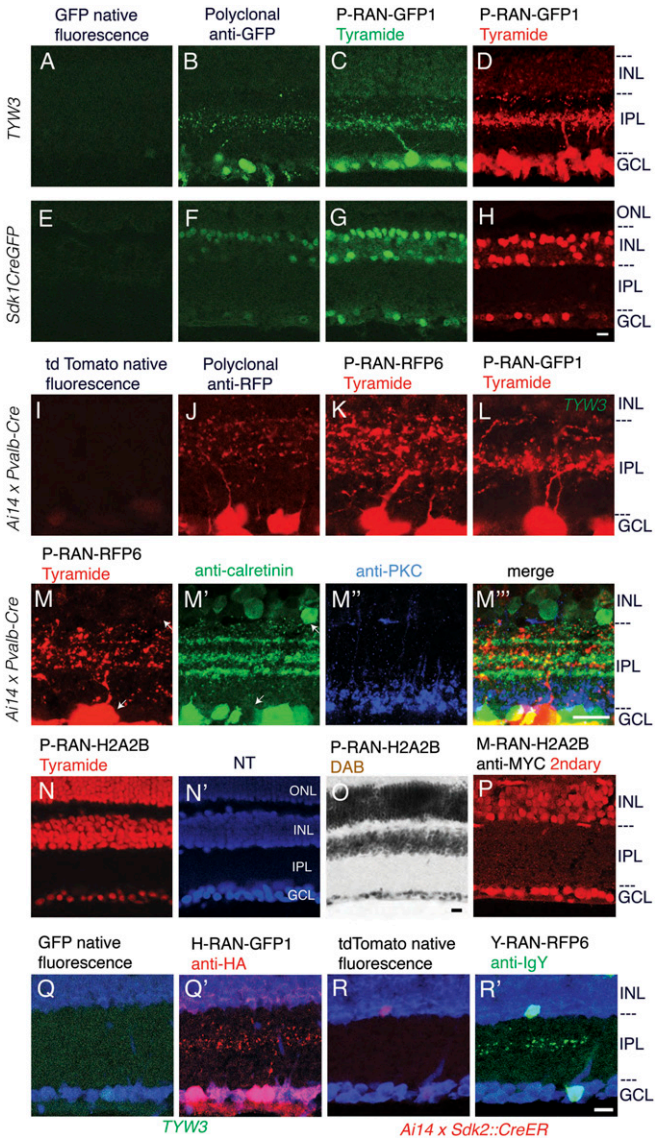


**Fig. 6.** Detection of antigens in tissue sections by RANbodies. (*A–D*) Sections of retina from a TYW3 mouse in which YFP is expressed in subsets of RGCs with dendrites in the central sublaminae of the inner plexiform layer. (*A*) Native fluorescence. (*B*) Chicken anti-GFP. (*C*) P-RAN-GFP1/FITC-tyramide. (*D*) P-RAN-GFP1/Cy3-tyramide. All images were obtained with the same gain. GCL, ganglion cell layer; INL, inner nuclear layer; IPL, inner plexiform layer; ONL, outer nuclear layer. (*E–H*) Sections of retina from a Sdk1::CreGFP mouse, stained as in *A–D*, in which CreGFP is localized to nuclei of subsets of cells in the ganglion cell layer and inner nuclear layer. (*I–K*) Sections of retina from a double transgenic mouse (cre-dependent tdTomato;Parvalbumin-cre) in which subsets of RGCs express tdTomato. Sections were stained with anti-RFP or P-RAN-RFP6/Cy3-tyramide. The RANbody stained dendrites more distinctly than the antibody. (*L*) TYW3 retina stained with P-RAN-GFP1 as in *A–D*, showing similarly distinct staining of dendrites. (*M–M‴*) Section of retina from a cre recombinase-dependent tdTomato;Parvalbumin-cre mouse stained with P-RAN-RFP6/Cy3-tyramide (*M*), rabbit anti-calretinin (*M′*), mouse anti-protein kinase C (PKC) (*M″*), and anti-rabbit and mouse secondary antibodies (*M‴*). RANbodies can be used together with conventional antibodies from multiple species. (*N*, *N′*, and *O*) Sections of wild-type mouse retina incubated with P-RAN-H2A2B and stained with Cy3-tyramide (*N*) plus NeuroTrace (*N′*) or with DAB (*O*). RAN-H2A2B stained all nuclei. (*P*) Section of wild-type mouse retina incubated with M-RAN-H2A2B and stained with anti-MYC. All nuclei are stained. (*Q* and *Q′*) Section of retina from an adult TYW3 mouse stained with H-RAN-GFP1 and Alexa 555-coupled mouse monoclonal antibody to HA tag. (*R* and *R′*) Section of retina from an adult Ai14;Sdk2::CreER stained with Y-RAN-RFP6 and Alexa488-conjugated anti-chicken IgY secondary antibodies. In both *Q* and *R*, neuronal processes in the inner plexiform layer (IPL) are clearly visible using RANbodies (*Q′* and *R′*), whereas native fluorescence from reporters (GFP and tdTomato) is inadequate to reveal these processes (*Q* and *R*). (Scale bar in *H*: 10 μm for *A–H*; scale bar in *M‴* :10 μm for *I–M‴* ; scale bar in *O*: 10 μm for *N–O*; scale bar in *R′*: 10 μm for *P–R′*.)

H-RAN-GFP26, the IgY-derived Y-RAN-GFP26 was able to detect GFP (Fig. 5*L*).

**Detection of Antigens with RANbodies in Tissue Sections.** Finally, we assessed the ability of RANbodies to stain tissue sections. We used mouse retina because we have characterized several transgenic lines in which retinal neurons express XFPs. P-RAN-GFP1 recognized GFP derivatives in each of two such lines tested. In TYW3, subsets of retinal ganglion cells (RGCs) express YFP cytoplasmically, revealing somata and dendrites of several distinct RGC types (34, 35). In Sdk1::CreGFP mice (*SI Materials and Methods*), CreGFP is localized to the nuclei of Sdk1-expressing cells, some of which have been characterized previously (36). Sections were treated with $H_2O_2$ to inactivate endogenous peroxidase-like activities and then were incubated with P-RAN-GFP1 and reacted with the tyramide substrate. In both lines, staining was more intense with RANbody than with conventional anti-GFP antibodies and fluorophore-conjugated second antibodies (Fig. 6 *A–H*). In our hands, Cy3-tyramide (red color) resulted in crisper staining with lower background than FITC-tyramide (Fig. 6 *C*, *D*, *G*, and *H*) and more sensitive staining than chromogenic DAB staining. Moreover, fine dendrites in the inner plexiform layer were more clearly visualized with P-RAN-GFP1 than by indirect immunofluorescence (Fig. 6*L*). Similarly, P-RAN-RFP6 stained tdTomato-positive cells in double transgenics (Parvalbumin-Cre mated to Ai14, a tdTomato reporter line) (37, 38). Again, RANbody staining was more intense and better defined than indirect immunofluorescence using anti-tdTomato (Fig. 6 *I–K*). The staining is compatible with immunohistochemistry using monoclonal or polyclonal antibodies with anti-mouse or -rabbit secondary antibodies (see, for example, Figs. 4 *A* and *M* and 6*M*). This compatibility increases the range of possibilities for labeling multiple antigens in a single cell or section.

We also stained mouse retina with P-RAN-H2A2B and observed strong, specific staining of nuclei (Fig. 6 *N* and *O*). Thus, RANbodies can be used to detect endogenous antigens in tissue.

Finally, we confirmed that RANbodies incorporating HA-based spaghetti monsters, an MYC-based spaghetti monster, and a chick IgY Fc fragment (H-, M-, and Y-RANbodies, respectively) could all be used to reveal antigens in tissue sections. Examples are shown in Fig. 6 *P–R*.

## Discussion

This paper describes RANbodies, versatile reagents generated by fusing a reporter to a nanobody. RANbodies can be used to detect antigens in cells and tissues. They are sensitive, because of the amplification provided by the reporters (enzymatic for HRP and incorporation of multiple epitopes in the spaghetti monsters); specific, because of the monoclonal nature of nanobodies; inexpensive, because they can be produced by standard methods in most laboratories; and eternal because they can be regenerated based on information contained in a simple digital sequence file. We show that they can be used to detect a variety of antigens in both cultured cells and tissue sections. In addition to detecting endogenous antigens (e.g., histones and gelsolin), they can be used to amplify the endogenous fluorescence of GFP, RFP, tdTomato, and mCherry, decreasing reliance on expensive commercial anti-XFP antibodies. Although we have not used them for superresolution or electron microscopy, they are very likely to be valuable reagents for these modalities as well.

We generated RANbodies incorporating four reporters, allowing visualization by using colorimetric and fluorescent enzymatic amplification (P series, HRP), commercially available

anti-epitope tag antibodies (H and M series, HA- and MYC-tagged spaghetti monsters, respectively), and second antibodies (Y series, chicken IgY). Each has advantages. The amplification provided by the enzymatic activity of HRP renders the P series many-fold more sensitive than standard indirect fluorescence. Moreover, no secondary antibody is required for detection. On the other hand, enzymatic reaction on tissue is sometimes cumbersome and requires careful monitoring of incubation time. In addition, the tyramide reagents used for fluorescent detection are expensive, and the inexpensive colorimetric substrates are incompatible with most multiple-labeling protocols. Conversely, H-, M-, and Y-RANbodies are simpler to use and are well suited for multiple labeling, but, although they are approximately as sensitive as standard indirect immunofluorescence, they are less sensitive than P-RANbodies. The Y-RANbodies have the additional advantage of enabling the use of anti-chicken second antibodies, which can be combined with more widely used anti-rodent and -rabbit secondary antibodies. For example, the best currently available antibodies to tdTomato, to our knowledge, are generated in rabbits and are therefore are difficult to combine with broadly available rabbit antibodies. Y-RAN-RFPs provide a useful alternative, increasing the range of antibodies that can be used in combination with RFP detection.

The advantages of nanobodies have been broadly appreciated: A search of PubMed with the term "nanobody OR nanobodies" retrieves 617 items in 2015–2017 alone. Thus, new nanobodies are being generated at a rapid rate. As nanobodies to additional antigens become available, the utility of the RANbody method is likely to increase.

## Materials and Methods

Animals were used in accordance with NIH guidelines and protocols approved by the Institutional Animal Use and Care Committee at Harvard University.

**Construction of RANbodies.** DNA sequences including a signal sequence from the human Ig kappa chain, an HA tag, codon-optimized HRP, and a His tag were assembled in a backbone of pCMV-N1-EGFP (Clontech) together with sequences encoding nanobodies which had been synthesized as gBlocks gene fragments (Integrated DNA Technology) using the Gibson Assembly HiFi 1-Step kit (SGI-DNA). In some cases, the synthesized nanobody sequences were inserted between the HA tag and HRP sequence after amplifying the vector sequence by PCR. In other cases, reporter sequences were inserted between the nanobody and His tag sequence. Sequences for nanobodies described in this report are presented in Table S1. RANbody constructs are available from Addgene.

**Production of RANbodies.** To produce RANbody proteins, 293T cells were transfected with RANbody plasmid DNA using a calcium phosphate precipitation method followed by 15% (wt/vol) glycerol shock in serum-free DMEM. After switching to DMEM10 or Opti-MEM I (Thermo Fisher/Invitrogen), the cells were incubated for 3 d. The medium, which contained secreted RANbody, was harvested, filtered through 0.45-μm-pore cellulose acetate membranes, and applied to cobalt Talon resin columns (Clontech), rinsed, and eluted according to the manufacturer's protocol. The eluate was concentrated using Pierce 9K concentrators (Thermo Fisher) and then substituted with several cycles of PBS. RANbodies were stored at 4 °C with 0.01% (vol/vol) ProClin 150 (Sigma-Aldrich) as a preservative or were aliquoted and frozen at −20 °C. In practice, it is possible to use cultured medium harvested after plasmid transfection without further purification.

Primer sequences, sources of reagents, and protocols for imaging, cell culture and biochemical assays are detailed in *SI Materials and Methods*.

**ACKNOWLEDGMENTS.** This work was funded by NIH Grant R37 NS029169.

1. Coons AH (1958) Fluorescent antibody methods. *Gen Cytochem Methods* 1:399–422.
2. Nakane PK, Pierce GB, Jr (1967) Enzyme-labeled antibodies for the light and electron microscopic localization of tissue antigens. *J Cell Biol* 33:307–318.
3. Ramos-Vara JA, Miller MA (2014) When tissue antigens and antibodies get along: Revisiting the technical aspects of immunohistochemistry–the red, brown, and blue technique. *Vet Pathol* 51:42–87.
4. Saper CB, Sawchenko PE (2003) Magic peptides, magic antibodies: Guidelines for appropriate controls for immunohistochemistry. *J Comp Neurol* 465:161–163.
5. Baker M (2015) Reproducibility crisis: Blame it on the antibodies. *Nature* 521:274–276.
6. Köhler G, Milstein C (1975) Continuous cultures of fused cells secreting antibody of predefined specificity. *Nature* 256:495–497.
7. Morrison SL (1992) In vitro antibodies: Strategies for production and application. *Annu Rev Immunol* 10:239–265.
8. Ma H, O'Kennedy R (2017) Recombinant antibody fragment production. *Methods* 116:23–33.
9. Hamers-Casterman C, et al. (1993) Naturally occurring antibodies devoid of light chains. *Nature* 363:446–448.
10. Greenberg AS, et al. (1995) A new antigen receptor gene family that undergoes rearrangement and extensive somatic diversification in sharks. *Nature* 374:168–173.
11. Nguyen VK, Desmyter A, Muyldermans S (2001) Functional heavy-chain antibodies in Camelidae. *Adv Immunol* 79:261–296.
12. De Meyer T, Muyldermans S, Depicker A (2014) Nanobody-based products as research and diagnostic tools. *Trends Biotechnol* 32:263–270.
13. Gonzalez-Sapienza G, Rossotti MA, Tabares-da Rosa S (2017) Single-domain antibodies as versatile affinity reagents for analytical and diagnostic applications. *Front Immunol* 8:977.
14. Rothbauer U, et al. (2006) Targeting and tracing antigens in live cells with fluorescent nanobodies. *Nat Methods* 3:887–889.
15. Ariotti N, et al. (2015) Modular detection of GFP-labeled proteins for rapid screening by electron microscopy in cells and organisms. *Dev Cell* 35:513–525.
16. Beghein E, Gettemans J (2017) Nanobody technology: A versatile toolkit for microscopic imaging, protein-protein interaction analysis, and protein function exploration. *Front Immunol* 8:771.
17. Traenkle B, Rothbauer U (2017) Under the microscope: Single-domain antibodies for live-cell imaging and super-resolution microscopy. *Front Immunol* 8:1030.
18. Viswanathan S, et al. (2015) High-performance probes for light and electron microscopy. *Nat Methods* 12:568–576.
19. Gibson DG, et al. (2009) Enzymatic assembly of DNA molecules up to several hundred kilobases. *Nat Methods* 6:343–345.
20. Porstmann B, Porstmann T, Nugel E, Evers U (1985) Which of the commonly used marker enzymes gives the best results in colorimetric and fluorimetric enzyme immunoassays: Horseradish peroxidase, alkaline phosphatase or beta-galactosidase? *J Immunol Methods* 79:27–37.
21. Schikorski T, Young SM, Jr, Hu Y (2007) Horseradish peroxidase cDNA as a marker for electron microscopy in neurons. *J Neurosci Methods* 165:210–215.
22. Morawski B, Quan S, Arnold FH (2001) Functional expression and stabilization of horseradish peroxidase by directed evolution in *Saccharomyces cerevisiae*. *Biotechnol Bioeng* 76:99–107.
23. Joesch M, et al. (2016) Reconstruction of genetically identified neurons imaged by serial-section electron microscopy. *eLife* 5:e15015.
24. Martell JD, et al. (2016) A split horseradish peroxidase for the detection of intercellular protein-protein interactions and sensitive visualization of synapses. *Nat Biotechnol* 34:774–780.
25. Kubala MH, Kovtun O, Alexandrov K, Collins BM (2010) Structural and thermodynamic analysis of the GFP:GFP-nanobody complex. *Protein Sci* 19:2389–2401.
26. Nagai T, et al. (2002) A variant of yellow fluorescent protein with fast and efficient maturation for cell-biological applications. *Nat Biotechnol* 20:87–90.
27. Jullien D, et al. (2016) Chromatibody, a novel non-invasive molecular tool to explore and manipulate chromatin in living cells. *J Cell Sci* 129:2673–2683.
28. Van den Abbeele A, et al. (2010) A llama-derived gelsolin single-domain antibody blocks gelsolin-G-actin interaction. *Cell Mol Life Sci* 67:1519–1535.
29. Fridy PC, et al. (2014) A robust pipeline for rapid production of versatile nanobody repertoires. *Nat Methods* 11:1253–1260.
30. Shaner NC, et al. (2004) Improved monomeric red, orange and yellow fluorescent proteins derived from *Discosoma sp.* red fluorescent protein. *Nat Biotechnol* 22: 1567–1572.
31. Feinberg EH, et al. (2008) GFP reconstitution across synaptic partners (GRASP) defines cell contacts and synapses in living nervous systems. *Neuron* 57:353–363.
32. Gordon MD, Scott K (2009) Motor control in a *Drosophila* taste circuit. *Neuron* 61: 373–384.
33. Yamagata M, Sanes JR (2012) Transgenic strategy for identifying synaptic connections in mice by fluorescence complementation (GRASP). *Front Mol Neurosci* 5:18.
34. Kim I-J, Zhang Y, Meister M, Sanes JR (2010) Laminar restriction of retinal ganglion cell dendrites and axons: Subtype-specific developmental patterns revealed with transgenic markers. *J Neurosci* 30:1452–1462.
35. Zhang Y, Kim I-J, Sanes JR, Meister M (2012) The most numerous ganglion cell type of the mouse retina is a selective feature detector. *Proc Natl Acad Sci USA* 109: E2391–E2398.
36. Krishnaswamy A, Yamagata M, Duan X, Hong YK, Sanes JR (2015) Sidekick 2 directs formation of a retinal circuit that detects differential motion. *Nature* 524:466–470.
37. Hippenmeyer S, et al. (2005) A developmental switch in the response of DRG neurons to ETS transcription factor signaling. *PLoS Biol* 3:e159.
38. Madisen L, et al. (2010) A robust and high-throughput Cre reporting and characterization system for the whole mouse brain. *Nat Neurosci* 13:133–140.